

AperTO - Archivio Istituzionale Open Access dell'Università di Torino

Temporal dynamics of the transmission of *Xylella fastidiosa* subsp. *pauca* by *Philaenus spumarius* to olive plants

This is a pre print version of the following article:

Original Citation:

Availability:

This version is available <http://hdl.handle.net/2318/1797421> since 2021-08-20T12:13:05Z

Published version:

DOI:10.1127/entomologia/2021/1294

Terms of use:

Open Access

Anyone can freely access the full text of works made available as "Open Access". Works made available under a Creative Commons license can be used according to the terms and conditions of said license. Use of all other works requires consent of the right holder (author or publisher) if not exempted from copyright protection by the applicable law.

(Article begins on next page)

1 **Temporal dynamics of *Xylella fastidiosa* subsp. *pauca* vector**
2 **transmission to olive plants**

3

4 ***Xylella* transmission by the meadow spittlebug (short title)**

5

6 Nicola Bodino¹, Vincenzo Cavalieri², Mattia Pegoraro¹, Giuseppe Altamura², Francesca Canuto¹,
7 Stefania Zicca², Giulio Fumarola³, Rodrigo P. P. Almeida⁴, Maria Saponari², Crescenza
8 Dongiovanni^{3*}, and Domenico Bosco^{1,5}

9 ¹ CNR–Istituto per la Protezione Sostenibile delle Piante, Strada delle Cacce, 73, 10135 Torino,
10 Italy

11 ² CNR–Istituto per la Protezione Sostenibile delle Piante, SS Bari, Via Amendola 122/D, 70126
12 Bari, Italy

13 ³ CRSFA–Centro di Ricerca, Sperimentazione e Formazione in Agricoltura Basile Caramia, Via
14 Cisternino, 281, 70010 Locorotondo (BA), Italy

15 ⁴ Department of Environmental Science, Policy and Management, University of California, 2000
16 Carleton Street, Berkeley, CA, USA

17 ⁵ Dipartimento di Scienze Agrarie, Forestali e Alimentari, Università degli Studi di Torino, Largo
18 Paolo Braccini, 2, 10095 Grugliasco (TO), Italy

19 *Correspondence: enzadongiovanni@crsfa.it, domenico.bosco@unito.it

20

21 **Abstract**

22 The spittlebug *Philaenus spumarius* L. (Hemiptera: Aphrophoridae) is the predominant vector of
23 *Xylella fastidiosa* Wells et al. (Xanthomonadales: *Xanthomonadaceae*) (*Xf*) to olive trees in the
24 Apulia Region of Italy. Previous studies focused on assessing *Xf* transmission competence by
25 spittlebugs and the natural infectivity of the *P. spumarius* populations. However, factors
26 influencing *Xf* transmission by *P. spumarius* are largely unknown and these knowledge gaps
27 hamper the comprehension of the epidemiology of *Xf*-associated emerging diseases. We
28 performed two sets of experiments to study transmission biology of *Xf* by *P. spumarius* aimed at
29 understanding the kinetics of the bacterial persistence, transmission efficiency and the spread rate
30 of *Xf* among olive trees in summer and autumn. The results show that i) *P. spumarius* is a
31 competent *Xf* vector to olive throughout its adult life, ii) bacterial load in the vector foregut
32 increases during the first 2-3 weeks after acquisition and then becomes stable, iii) transmission
33 rates may significantly vary during the year and under different climatic conditions, and iv)
34 differential survival of vectors — influenced by insect age, season and climatic conditions —
35 may affect the spread of *Xf* in olive plants. Transmission parameters of *Xf* by *P. spumarius*
36 obtained here will improve the modelling of the pathogen spread, by explicitly incorporating the
37 effect of insect vectors, and the designing of effective control and prevention measures against
38 this vector-borne disease.

39

40 **Keywords**

41 vector-borne disease, vector bacterial load, Olive Quick Decline Syndrome, OQDS,
42 Aphrophoridae, spittlebugs, non circulative-persistent transmission.

43

44 **Introduction**

45 Transmission biology is of major importance in outlining disease epidemiology of insect-borne
46 plant pathogens (Jeger et al. 1998; Daugherty and Almeida 2009), and its detailed knowledge is a
47 key to elaborate effective disease management (Almeida et al. 2005). Transmission of pathogens
48 by insect vectors is a complex process characterized by several steps and actors, that involve
49 different areas of knowledge, including molecular biology, physics, physiology, and ecology
50 (Killiny et al. 2009; Sicard et al. 2018; Ranieri et al. 2020; Backus and Shih 2020). Ultimately,
51 the most fundamental characteristic of vector transmission – especially from a disease control
52 perspective – is efficiency or competence, i.e. how often a vector transmits a pathogen over time
53 or per transmission opportunity (Purcell and Almeida 2005). Transmission efficiency of persistent
54 plant pathogens by insect vectors may significantly vary over time after acquisition, and it is a
55 process influenced by the host condition and environmental factors (Anhalt and Almeida 2008;
56 Daugherty et al. 2009; Ghanim 2014; Daugherty and Almeida 2019). Nonetheless,
57 epidemiological models rarely explicitly include these aspects, often because of the lack of
58 reliable estimates of key parameters of vector transmission of pathogens. These limitation lead
59 biases in the outcomes and predictions of disease dynamics models (Jeger 2000; Allen et al.
60 2019).

61 The meadow spittlebug, *Philaenus spumarius* L. (Hemiptera: Aphrophoridae), is the key vector
62 of the exotic bacterium *Xylella fastidiosa* Wells et al. (Xanthomonadales: *Xanthomonadaceae*)
63 (*Xf* hereafter) in Italy and Europe (Cornara et al. 2018, 2019). *Xf* subsp. *pauca* is associated to the
64 most severe *Xf*-epidemic currently affecting Europe, being the causal agent of the olive quick
65 decline syndrome (OQDS) in Apulia (South Italy) (Saponari et al. 2019). In this region, this
66 introduced bacterium encountered large populations of a previously neglected xylem-sap feeder

67 insect, *P. spumarius*, and a landscape dominated by susceptible olive plants leading to a dramatic
68 epidemic that wiped away in less than one decade the olive production in the infected area
69 (Saponari et al. 2019; Schneider et al. 2020). Ongoing research on *Xf* in Europe has revealed that
70 the *P. spumarius* i) is the dominant xylem-sap feeder in olive agroecosystem and Mediterranean
71 region (Morente et al. 2018; Antonatos et al. 2019; Bodino et al. 2019), ii) adults are found
72 naturally infected with *Xf* in olive groves during summer and autumn (Cornara et al. 2017b;
73 Cavalieri et al. 2019), and iii) is able to transmit the bacterium from olive-to-olive and from other
74 plants to olive in laboratory trials (Cornara et al. 2017a, 2020; Cavalieri et al. 2019).

75 Current knowledge on *Xf* transmission biology comes from American pathosystems – e.g.
76 diseases of grapevine and citrus – where sharpshooters (Hemiptera: Cicadellidae: Cicadellinae)
77 represent the main group of vectors (Redak et al. 2004; Esteves et al. 2018; Cornara et al. 2019).
78 Once acquired through feeding in xylem vessels colonized by *Xf*, bacterial cells multiply in the
79 foregut of the insect vector and are persistently transmitted in a noncirculative manner, with no
80 transtadial or transovarial passage and no apparent latent period (Severin 1950; Freitag 1951;
81 Purcell and Finlay 1979). Acquisition and inoculation efficiency of *Xf* may vary greatly according
82 to several factors — e.g. vector species (Daugherty and Almeida 2009; Marucci et al. 2008),
83 source or recipient plant species and tissue, conditions of the host plants (water stress, disease
84 symptoms) (Daugherty et al. 2011; Krugner et al. 2012; Krugner and Backus 2014), season and
85 climate conditions (Daugherty et al. 2009, 2017) — shaping vectors' feeding preferences and
86 acquisition rates (Almeida et al. 2005; Gruber and Daugherty 2013).

87 Despite its importance in affecting epidemics spread and severity, several aspects of the
88 transmission biology of *Xf* by *P. spumarius* on olive trees have not been investigated, since the
89 previous studies on the Apulian pathosystem focused on assessing the transmission capability of

90 spittlebugs. In addition, some information inferred from American pathosystems may not be
91 directly transferable to the Italian olive disease, given the differences (e.g. vector species, *Xf*
92 genotypes, host plants) that affect transmission parameters and inoculation efficiency (e.g.
93 Almeida et al. 2005; Esteves et al. 2018). A better knowledge on *Xf* transmission parameters of
94 European vectors is therefore necessary, allowing epidemic models to take into account pathogen
95 transmission dynamics, so far not explicitly incorporated in any of the proposed models of *Xf*
96 spread in Europe (White et al. 2017, 2020; Strona et al. 2020).

97 The aim of this work was to study *Xf* subsp. *pauca* kinetics in *P. spumarius* over time and *Xf*
98 transmission efficiency by *P. spumarius* to olive trees throughout the year. We investigated how
99 acquisition, bacterial load, and transmission efficiency are affected by season, climatic
100 conditions, and the duration of plant exposure to infectious vectors. More specifically, we carried
101 out experiments at different times of the year to determine i) *Xf* persistence, population size in the
102 foregut of *P. spumarius*, ii) pathogen transmission success to olive seedlings after different
103 periods post acquisition, and iii) *Xf* spread by infected spittlebugs within an experimental
104 population of olive seedlings under different climatic conditions.

105 **Materials and Methods**

106 **Insects and plants**

107 *P. spumarius* adults were field collected in dry meadows and olive groves located in *Xf*-free areas
108 of Apulia (southern Italy) one to two weeks prior to the onset of each experimental assay, and
109 maintained in mesh and plastic fabric cages (Bugdorm: 75x75x115 cm) containing potted host
110 plants (*Medicago sativa*, *Vitis vinifera*, *Sonchus oleraceus*, *Vicia faba*, *Erigeron* spp.). The cages
111 were placed in a climatic chamber (24.7 ± 1.0 °C, $72.1 \pm 7.2\%$ RH) in summer and at a shaded

112 location during autumn in the nursery “Li Foggi” of ARIF (Agenzia Regionale Attività Irrigue e
113 Forestali) (Gallipoli, province of Lecce). The air temperature and relative humidity were recorded
114 hourly in both conditions using data loggers (HOBO U23-002; Onset Computer, Bourne, MA,
115 USA). Adult mortality was low (5–10% of total insects collected). To confirm the *Xf*-free status
116 of the reared spittlebugs, before starting each acquisition assays, 20-30 individuals were collected
117 and individually tested by real time PCR (qPCR). No positive individuals were detected.

118 Recipient olive plants used for all experiments consisted of certified pathogen-free olive
119 seedlings produced and maintained in the facilities of the Premultiplication Center at CRSFA.
120 Seedlings of about 20–30 cm in height (6–8 months old) with active growing apexes were
121 selected and transferred at the nursery “Li Foggi” of ARIF just before starting each experiment.

122 **Kinetics of *Xf* colonization of *P. spumarius* and transmission efficiency**

123 Olive-to-olive transmission efficiency, *Xf* retention and multiplication in *P. spumarius* adults were
124 tested in four separate assays carried out in 2017-2018 in different seasons, allowing us to
125 investigate the effects of time after pathogen acquisition access period (hereafter AAP), season
126 (summer: late June-July; autumn: late September-November) and insect age on the transmission
127 parameters. Acquisition of *Xf* by *P. spumarius* adults was performed by caging the insects on
128 branches of naturally infected olive trees (4–5 years old, cv. “Cellina di Nardò”) located in olive
129 groves in the municipalities of Gallipoli and Parabita (province of Lecce). Branches suitable for
130 acquisition were first tested by qPCR (approx. two weeks before the AAP) to assess for the
131 presence and abundance of *Xf* in young flushes. Source plants hosted bacterial populations
132 ranging from a median value of 8.99×10^5 (IQR: $1.41 \times 10^5 - 1.99 \times 10^6$) CFU/g in summer to
133 1.88×10^5 (IQR: $1.22 \times 10^5 - 2.41 \times 10^5$) CFU/g in autumn. Considering separately young and
134 mature leaves from the branches selected for acquisition, the median bacterial populations ranged

135 from of 2.06×10^5 (IQR: $7.69 \times 10^4 - 9.15 \times 10^5$) CFU/g of tissue in young leaves to 1.5×10^6
136 (IQR: $5.06 \times 10^5 - 3.98 \times 10^6$) in mature leaves. *Philaenus spumarius* adults from maintenance
137 cages were isolated — enclosed in mesh sleeves — on a total of 10–12 *Xf*-positive branches of 6–
138 12 field-grown olives for an AAP of three days (72h), in groups of 50–100 individuals per
139 branch.

140 At the end of the AAP spittlebug cohorts were mixed and transferred to a post-AAP maintenance
141 period in five new cages containing potted non-host plants of *Xf* subsp. *pauca*, according to
142 EFSA (2018) (Bugdorm: 75x75x115 cm and 45x45x90; *V. vinifera*, *S. oleraceus*, *V. faba*, *Pistacia*
143 *lentiscus* and *Vicia sativa*). Inoculation assays were carried out using insects randomly collected
144 from maintenance cages at different timepoints after the AAP (Supplementary Tab. 1) and
145 transferred onto testing plants (i.e. olive seedlings) for an inoculation access period (hereafter
146 IAP) of three days (72 h). Each replica consisted of one potted olive seedling enclosed in a mesh
147 sleeve, on which five *P. spumarius* individuals were confined, thus having access to the entire
148 plant during IAP. Five replicas at each time point after AAP were carried out, for a total of 25
149 insects used for each inoculation assay. At some time points post-AAP insects were collected
150 from maintenance cages and stored directly in ethanol, for qPCR estimates of bacterial load (see
151 Supplementary Tab. 1). AAP and IAP duration (72h each) were chosen on the basis of both
152 preliminary trials and previous studies (Cavaliere et al. 2019) in order to maximize transmission
153 efficiency and insect survival. Both IAP assays and post-AAP rearings took place in the climatic
154 chamber located at the above-mentioned nursery “Li Foggi” at 24.7 ± 1.0 °C and 72.1 ± 7.2 % RH
155 in summer and 20.8 ± 1.0 °C and 77.9 ± 7.6 % RH in autumn. At the end of IAP, both live and dead
156 insects were collected, and singly stored in ethanol 90% at -20 °C. Insect survival rate was
157 recorded for each AAP and IAP assay. Recipient plants were treated with a systemic insecticide

158 (Imidacloprid, Confidor 200 SL) and kept in an insect-proof screenhouse. Olive test plants were
159 analysed for *Xf* both at 6 and 12 months after the experimental assays. Plants testing positive at
160 the first assay (6 months) were always positive at the second assay (12 months).

161 **Spread of *Xf* by *P. spumarius* under microcosm conditions**

162 Experimental assays in microcosms were carried out to assess influence of i) IAP duration, ii)
163 climatic conditions (semi-field vs controlled), and iii) season on the spread of *Xf*-infection within
164 an olive seedling population. The experiments were conducted in the same periods of the
165 transmission kinetic assays, i.e. summer (July) and autumn (September-October) for two
166 consecutive years (2017-2018). *Xf* acquisition by *P. spumarius* adults followed the same
167 procedure described above. At the end of 72h AAP, insects were collected from olive branches
168 and randomly transferred into mesh cages with wood frame (microcosms) (93 × 47.5 × 47.5 cm)
169 containing 16 olive seedlings each, positioned at regular spacing. In each microcosm 17
170 individuals were introduced in 2017 assays, and 32 individuals in 2018 assays. Spittlebugs were
171 released in the centre of the microcosm with a falcon tube, gently shaken until all insects left the
172 tube. To test the effect of climatic conditions, one set of cages (n = 12) was set up in controlled
173 climatic conditions (summer: 24.9 ± 1.9 °C, 74.5 ± 7.8% RH; autumn 22.4 ± 0.7 °C, 82.9 ± 6.4 %
174 RH), while another set (n = 12) was set up under semi-field climatic conditions, under a pine
175 shadowed area inside the above-mentioned nursery “Li Foggi” (summer: 26.3 ± 5.40 °C, 64.4 ±
176 22.5 % RH; autumn: 17.5 ± 3.9 °C, 63.3 ± 4.2 % RH). Climatic conditions were monitored using
177 dataloggers with probe inserted inside a randomly chosen microcosm. Insects were caged in each
178 set of microcosms for different IAP durations: 3-7-14-21 days, each with three independent
179 replicates (i.e. 3 single microcosms at each IAP per climatic condition). Olive seedlings were
180 watered during the assays every two days through individual drip irrigation, avoiding

181 disturbances to insects. All spittlebugs found inside the microcosms at the end of IAP, both live
182 and dead, were collected and stored in ethanol 90% at -20 °C. Insect survival rate was recorded
183 for each microcosm at the end of the IAP. Then, recipient olive seedlings were treated with
184 imidacloprid and kept in an insect-proof greenhouse. Test plants were analysed for *X. fastidiosa*
185 6 and 12 months after the experimental assay. Plants testing positive at the first assay (6 months)
186 were always positive at the second assay (12 months), when in average 30% more plants tested
187 positive.

188 ***Xf* detection in insects**

189 The insect head was removed using needles and a stereomicroscope. Each single head was then
190 homogenized in CTAB buffer with a tungsten carbide bead (7mm in diameter) using the Mill300
191 mixer (Qiagen, Germany). Homogenized samples were incubated at 65°C for 30min prior to be
192 treated with an equal volume of chloroform - isoamyl alcohol (24:1) followed by a 2-propanol
193 precipitation. The pellet recovered was eluted in 30µl of sterile water. One microliter of the
194 purified DNA was used to set up the real-time qPCR reactions (12,5 µl final volume) using the
195 specific primers and the TaqMan probe described in Harper et al. (2010). To estimate the bacterial
196 populations in the tested insect samples, a 10-fold serial dilution of *X. fastidiosa* cultured cells,
197 from 10⁶ CFU/ml to 10² CFU/ml, was included in all assays. The mean number of *Xf* cells in
198 amplified samples was automatically calculated by CFX Maestro TM Software (Bio-Rad).
199 Samples yielding doubtful qPCR results were re-amplified in direct and nested PCR assays
200 targeting the *holC* gene according to Cruaud et al. (2018). The samples displaying the specific
201 band on agarose gel were then considered positive.

202 ***Xf* detection in plants**

203 Branches for caging the insects for field acquisition of *Xf* were selected, marked and two leaf
204 samples collected: one including 6–8 leaves collected from the apical part of the shoots (within
205 the last 5–8cm) and the second one including 6–8 mature leaves collected from the basal part of
206 the shoots. Petioles and midribs were recovered from each samples and homogenized in CTAB
207 buffer (1:10 w:v). An aliquot of 1ml of the recovered plant sap was then processed following the
208 standard CTAB protocol (EPPO 2019). Real time PCR reactions for the detection and
209 quantification of the bacterium in these samples were set up as previously described for the
210 insects. For testing the recipient plants, 4–6 leaves were detached from the seedlings and
211 processed as described above. All the recipient plants were tested twice: a first screening
212 performed 6 months after the IAP (data not shown) and then a final assessment at 12 months after
213 the IAP.

214 **Statistical analysis**

215 The proportion of *Xf*-positive *P. spumarius* and the proportion of infected olive seedlings in the
216 kinetic experiment were separately modelled by logistic GLMM (binomial link) with *Time post-*
217 *acquisition*, *Season* and their interaction as fixed covariates and *Year* as random intercept. The *Xf*
218 population size in infected *P. spumarius* individuals throughout the kinetic experiment was
219 analysed separately for each assay by both linear regression and Michaelis-Menten (M-M) (1)
220 models:

$$221 \quad y = \frac{ax}{(b+x)}, \quad (1)$$

222 where *a* and *b* are model coefficients, *y* represents number of *Xf* cells in the insect head, and *x*
223 represents days after AAP beginning. Models fit was compared by Akaike's Information

224 Criterion corrected for small sample size (AIC_c). In all tests, *Xf* population size was decimal log
225 transformed to meet model assumptions. The proportion of infected olive plants was analysed by
226 logistic GLM (binomial link) as a function of fixed covariates *Mean Xf population size in vector*
227 *batch*, *Number of Xf-positive individuals in inoculation batch* and *Season*. Efficiency of
228 transmission by *P. spumarius*, i.e. inoculation rate, was estimated using two non-linear functions
229 derived from binomial probability model and Poisson probability model, respectively (Purcell
230 1981; Daugherty and Almeida 2009):

$$231 \quad P_{NB} = 1 - (1 - ba)^{NB} , \quad (2)$$

$$232 \quad P_{NB} = 1 - e^{-baNB} , \quad (3)$$

233 where N is the number of vectors, B is the IAP duration, a is the probability that a vector is
234 infected, and b is the vector inoculation rate. N and B were fixed parameters in our study (5
235 insects, 3 days), and both a and P_{NB} were known for each vectors batch, given that insects and
236 inoculated plants were individually PCR-tested for *Xf*. The constant b , vector inoculation rate,
237 was the only parameter to be estimated, fitting (2) and (3) to the kinetic dataset using non-linear
238 least-squares regression (*nls* function). We then compared the over-all fit of both models using
239 Akaike's information criterion (AIC).

240 The proportion of *Xf*-positive *P. spumarius* in spread rate experiment was modelled for 2018
241 assays only, due to the low number of insects recaptured in 2017 assays, with *Inoculum duration*,
242 *Climatic conditions*, *Season*, and their interactions using binomial GLM (proportion). The *Xf*
243 population size in insects (decimal log transformed) was analysed by ANOVA using both full
244 dataset (PCR-positive and -negative individuals) and a subset of PCR-positive insects only. The
245 proportion of infected olive seedlings was analysed using full dataset (2017 + 2018) with
246 binomial GLMM with *Inoculum duration*, *Climatic conditions*, *Season*, *Year* and their

247 interactions, with replica, i.e. single microcosm, as random intercept. Survival rate of *P.*
248 *spumarius*, i.e. number of alive individuals at the end of IAP, was analyzed by binomial GLMM
249 as a function of fixed covariates *Inoculation duration*, *Climatic condition* and *Season*, with *Year*
250 as random intercept. All analyses were performed in R 4.0.3 (R Core Team 2020), with packages
251 *lme4* (Bates et al. 2015), *nlme* (Pinheiro et al. 2020), and *ggplot* (Wickham 2016).

252 **Results**

253 ***Xf* transmission kinetics of *P. spumarius* from olive to olive**

254 ***Xf* acquisition and retention**

255 The overall survival rate of spittlebugs isolated after a 3-day IAP on olive seedlings was 77.1%
256 (343 of 445 individuals), survival of *P. spumarius* isolated on olive seedlings was similar among
257 the assays and time periods post-AAP, with an interquartile range (IQR hereafter) between 60%
258 and 84%. The prevalence of *Xf*-positive insects varied at different timepoints after acquisition and
259 among assays. Overall, cumulative diagnostic results at different times post-AAP showed a
260 proportion of 50% of *Xf*-positive insects (276 positives on 553 tested). The interaction of the
261 fixed effects *Time post-AAP* and *Season* on the proportion of *Xf*-infected *P. spumarius* was
262 significant (*Season* × *Time post-AAP*: $\chi^2_1 = 8.03$, $P = 0.004$) (Tab. 1). That is, the proportion of
263 *Xf*-infected *P. spumarius* was higher in autumn (55–83%), compared to summer assays (20–
264 60%), during the first days post-acquisition (Fig. 1). Then, the proportion of *Xf*-infected insects
265 decreased overtime post-AAP in autumn assays (down to 40–50%), while in summer assays it
266 remained quite stable or slightly increased (30–60%) during the whole period post-AAP, up to 78
267 days (Fig. 1). The two sexes had the same proportion of *Xf*-positive individuals [males = 0.455
268 (76/167), females = 0.541 (190/351)] ($\chi^2_1 = 0.52$, $P = 0.471$).

269 ***Bacterial load in the insects***

270 *Xf* populations in *P. spumarius* foregut varied from a few hundred to a few thousand of cells
271 (IQR: 70–3500 cells/insect, median 836 cells/insect). 10% of positive insects hosted more than
272 10^4 cells in their mouthparts, with one extreme value of 1.2×10^5 . Bacterial load of infected *P.*
273 *spumarius* was not constant, but increased significantly overtime post-AAP, i.e. the slope
274 parameter *a* of M-M model was always significantly different from zero, and greater in autumn
275 than in summer assays, indicating that *Xf* population in vectors increased faster in autumn than in
276 summer (M-M model summer 2018: $a = 3.02 \pm 0.19$, $t = 15.61$, $P < 0.001$; M-M model autumn
277 2018: $a = 3.64 \pm 0.21$, $t = 17.58$, $P < 0.001$) (Fig. 2). *Xf* load during the first days after
278 acquisition, i.e. 3–9 days after start of the AAP, consisted in a few hundreds of cells (70–600 cells
279 per insects). *Xf* load increased overtime, reaching 10^3 – 10^4 cells per insect approximately between
280 13th and 20th day post-AAP (Fig. 2). The growth of *Xf* population in insects was slightly better
281 explained by the Michaelis-Menten model than the linear model in summer assays and in autumn
282 2018 assay (summer 2017: $AIC_{\text{linear}} = 79.5$, $AIC_{\text{M-M}} = 79.4$; summer 2018: $AIC_{\text{linear}} = 399.3$,
283 $AIC_{\text{M-M}} = 393.0$; autumn 2018: $AIC_{\text{linear}} = 358.4$, $AIC_{\text{M-M}} = 356.6$), while in autumn 2017 assay
284 the growth of *Xf* population was better described by the linear model, probably because the assay
285 ended earlier than in 2018, and *Xf* population did not reach a plateau ($AIC_{\text{linear}} = 260.2$, $AIC_{\text{M-M}} =$
286 262.9). In 2018 assays the estimated asymptote of mean number of *Xf* cells in the foregut of
287 infected *P. spumarius* was different between summer (2,455 cells, CI = 441–2,698) and autumn
288 (4,335 cells, CI = 1,729–12,543) assay, with plateau reached around 20 days after acquisition
289 (Fig. 2). However, in summer 2018 there were PCR-positive insects with low number of *Xf* cells,
290 i.e. 20–50, even at 60–78 days post-AAP.

291 *Xf* transmission to olive

292 Following acquisition from field-grown *Xf*-infected olives, *P. spumarius* adults were transferred
293 to olive seedlings for 3-day IAP for up to 78 days post-AAP in summer 2018 assay. Overall, 29
294 of 82 olive seedlings were positive for *Xf* (35.4%). Percentage of *Xf*-positive olive seedlings 12
295 months after inoculation, i.e. a proxy of inoculation success of *Xf* by *P. spumarius*, was variable
296 among assays and time post-AAP, the IQR was between 21% and 57% of tested olives infected
297 (Fig. 3). The proportion of infected PCR-tested olive seedlings was not significantly affected by
298 either *Time post-AAP* ($\chi^2_1 = 0.33$, $P = 0.856$), *Season* ($\chi^2_1 = 0.77$, $P = 0.378$) or their interaction
299 ($\chi^2_1 = 0.69$, $P = 0.403$) (Tab. 1). That is, inoculation rate was constant — and randomly variable
300 — across samples, with an average inoculation rate of 34%. The likelihood of *Xf* transmission to
301 olives increased significantly as the average *Xf* population in insects augmented, regardless of
302 season (*Xf* population: $\chi^2_1 = 5.72$, $P = 0.017$; *Season*: $\chi^2_1 = 0.50$, $P = 0.479$) (Supplementary Tab.
303 2). In other words, the larger the mean *Xf* population in *P. spumarius* individuals, the higher the
304 probability of successful pathogen transmission (Fig. 4). Conversely, the number of *Xf*-positive
305 insects did not significantly affect the likelihood of *Xf* transmission on olives, i.e. olive seedlings
306 inoculated with higher number of *Xf*-positive insects (range: 1-4 positive insects/batch) were not
307 significantly more likely to get infected than those inoculated with fewer infected insects
308 (*Number of Xf-infected insects*: $\chi^2_1 = 1.05$, $P = 0.306$) (Supplementary Tab. 2). Although not
309 statistically significant, the relationship between the number of positive insects and the successful
310 transmission showed an apparent trend, being a recipient olive seedling exposed to four *Xf*-
311 positive *P. spumarius* in average 2.6-fold more likely of infection compared to one exposed to a
312 batch containing a single positive insect.

313 ***Inoculation rate estimates***

314 Poisson model provided better fit to the kinetic transmission dataset than binomial model, based
315 on AIC score. Overall vector inoculation rate b (proportion/vector/day), estimated from Poisson
316 model, was 0.062 ± 0.014 ($t_{16} = 4.44$, $P < 0.001$) when pooling all the assays performed during
317 different seasons. Considering separately the assays performed in summer and autumn provided
318 different estimates, lower in summer (0.034 ± 0.015 , $t_8 = 2.24$, $P = 0.05$) than in autumn ($0.08 \pm$
319 0.02 , $t_7 = 4.06$, $P = 0.005$).

320 **Spread of *Xf* by *P. spumarius* under microcosm conditions**

321 Overall, recapture rate of alive *P. spumarius* from microcosms at the end of IAPs, i.e. survival
322 rate, was 48% (1,127 alive out of 2,352 insects released). Survival of insects in microcosms was
323 affected by both the interaction of IAP duration and season (*IAP duration* \times *Season*: $\chi^2_1 = 26.87$,
324 $P < 0.001$), and the interaction of season and climatic conditions (*Season* \times *Climatic condition*:
325 $\chi^2_1 = 6.43$, $P = 0.011$) (Tab. 2). Therefore, lower survival rate was recorded at the end of longer
326 IAPs, especially during autumn assays, e.g. at the end of 21-days long IAPs only 3% (2017) and
327 4% (2018) of insects released inside microcosms were collected alive, irrespective of the climatic
328 condition. Survival rate of caged *P. spumarius* was higher in summer, especially in controlled
329 climatic conditions (2017: 66.7%, 2018: 85.2%) than in semi-field conditions (2017: 28.9%,
330 2018: 49.2%).

331 Effects of season, days after AAP, and climatic conditions on the proportion of infected *P.*
332 *spumarius* were analyzed for 2018 assays only, given the low number of infected insects
333 recollected during 2017 assays ($n = 32$, 3.9%). In 2018 assays there was a significant interaction
334 among the three covariates — *IAP duration*, *Season*, and *Climatic condition* — on the proportion

335 of infected insects recaptured ($\chi^2_1 = 8.78$, $P = 0.003$) (Tab. 2). That is, the proportion of infected
336 *P. spumarius* was initially lower in summer (IQR: 31-35%) than in autumn (IQR: 66-77%), then,
337 during summer, it slightly decreased overtime both in controlled and semi-field conditions, while
338 in autumn the proportion of infected *P. spumarius* abruptly decreased at longer IAPs in semi-field
339 conditions, and remained quite stable in controlled climatic conditions (Fig. 5).

340 Given the low number of positive insects recaptured in 2017 assays ($n = 32$), *Xf* population in
341 PCR-positive *P. spumarius* was analyzed only for 2018 assays ($n = 444$). PCR-positive
342 individuals had in average higher *Xf* population after longer IAPs (that is to say longer post-AAP
343 period) (*IAP duration*: $F_{1,375} = 8.75$, $P = 0.003$). Moreover, *P. spumarius* in the autumn assay had
344 higher mean *Xf* loads than those tested in summer (*Season*: $F_{1,375} = 35.49$, $P < 0.001$)
345 (Supplementary Tab. 3). Considering the total of recollected insects (both PCR-positive and -
346 negative individuals) in 2018 assays ($n = 957$), mean *Xf* population was higher in autumn, as
347 expected by the higher rate of positive insect (*Season*: $F_{1,696} = 10.13$, $P = 0.001$) (Tab. 2).
348 However, significant interaction was observed among *Season*, *Climatic condition*, and *IAP*
349 *duration* ($F_{1,696} = 8.38$, $P = 0.004$), that is, average *Xf* population in insects collected alive at the
350 end of IAP in autumn was high in both conditions at shorter IAPs, then gradually declined in
351 semi-field conditions, while in controlled conditions it remained stable; on the other hand, in
352 summer assay mean *Xf* population gradually declined in both conditions (Fig. 6).

353 ***Trasmission to olive***

354 Transmission rate, i.e. proportion of infected olive seedlings, was affected by *Climatic condition*
355 ($\chi^2_1 = 10$, $P = 0.001$), *Year* ($\chi^2_1 = 23.3$, $P < 0.001$), with significant interactions between *Climatic*
356 *condition* \times *Year* ($\chi^2_1 = 6.5$, $P = 0.011$) and *IAP duration* \times *Season* ($\chi^2_1 = 7.17$, $P = 0.007$) (Tab.
357 2). The proportion of infected olive seedlings was higher after longer IAPs in Autumn, and higher

358 in controlled conditions than in semi-field conditions, especially in 2017 trials (2017: 10-fold
359 higher likelihood of becoming infected compared to plants in controlled conditions, 2018: 1.5-
360 fold). Infection rates were higher in 2018 than in 2017 assays (plants had a 34-fold higher
361 likelihood of becoming infected in 2018), as partially expected given the higher number of
362 insects released in microcosms in 2018 compared to 2017 assays (32 and 17, respectively) (Fig. 7
363 and Tab. 2). That is, infection spread among olives increased with inoculation time in late season
364 only, especially in controlled climatic conditions and with higher vector density.

365 **Discussion**

366 We studied aspects of *Xf* transmission biology by *P. spumarius* on olive plants in order to shed
367 light on the epidemiology of this invasive bacterium in Europe and associate emerging diseases.
368 Two different sets of experiments were carried out in order to gain information on the influence
369 of post-acquisition time, seasonal, and climatic conditions on transmission efficiency, persistence,
370 and multiplication of *Xf* in the vector, as well as on survival of the insect vector. Our results
371 suggest that i) *P. spumarius* is a competent vector of *Xf* on olive throughout its adult life, ii) *Xf*
372 acquisition rate by the vector under field conditions varies between seasons, iii) the bacterium
373 load in vector's foregut increases during the first 2-3 weeks after acquisition, then becomes
374 stable, iv) the transmission rate to olive seedlings remains constant at different post-acquisition
375 times, but tends to increase with longer inoculation time (although differently among seasons and
376 climatic conditions), v) insect survival is influenced by age, season and climatic conditions,
377 affecting the transmission outcome in microcosm experiments, and possibly influencing the
378 spreading rate of *Xf* in olive groves.

379 Unexpectedly, the higher acquisition rate of *Xf* by *P. spumarius* in autumn compared to summer
380 assays did not follow a corresponding increase in *Xf* populations in the olive source plants, while
381 the acquisition rate of *Xf* by xylem-sap feeders is usually related to the population of the
382 bacterium in host plant (Hill and Purcell 1997). In our experiments, the estimated *Xf* loads in
383 source plants were slightly higher in summer than autumn, contrary to the expectation that *Xf*
384 population in plant tends to increase during the vegetative season (Hill and Purcell 1997;
385 Giampetruzzi et al. 2020). This discrepancy may be due to the sample collection of leaf tissues,
386 which in summer included mature leaves produced on shoots of the previous year, and thus
387 possibly harboring higher number of *Xf* cells — dead or alive — than in late season samples,
388 whereas sampling in autumn included mature leaves from shoots grown during the same year and
389 thus less heavily colonized by *Xf*. Alternatively, the limited number of leaves/branch used in our
390 tests may explain the results, given the heterogeneous distribution of *Xf* in the infected plants.

391 Once acquired, *Xf* multiplied in the foregut of *P. spumarius* reaching an average of a few
392 thousand cells after 2–3 wks, although in some individuals *Xf* population was estimated
393 exceeding forty thousand cells. The increase in *Xf* population was faster, and the plateau and the
394 maximum number of cells higher in autumn than it was in summer assays. The maximum number
395 of *Xf* cells in *P. spumarius* foregut was higher than the estimates made in previous studies, which
396 tested *Xf* population in the vector only after a few days post-acquisition (Cavalieri et al. 2019), or
397 in field-collected individuals, whose acquisition conditions are unknown (Cornara et al. 2017a),
398 or exposed to different *Xf* subspecies/host plant combination (e.g. *Xf. subsp. fastidiosa* in
399 grapevine) (Cornara et al. 2016). Indeed, our estimates for *Xf* population in the vector after eight
400 days after the start of AAP were similar to those tested at approximately the same time after
401 beginning of acquisition by Cavalieri et al. (2019), i.e. 400-900 cells. Moreover, the population

402 size measured in the head of *P. spumarius* in this work is compatible with the number of *Xf* cells
403 potentially hosted by *P. spumarius* estimated based on the cuticular surface available in foregut (\approx
404 67,000 cells) (Ranieri et al. 2020). Thus, our results show that *P. spumarius* can harbor in its
405 foregut *Xf* loads similar to the ones measured in the main sharpshooter vectors in America, e.g. *G.*
406 *atropunctata* and *H. vitripennis* (Hill and Purcell 1995; Almeida and Purcell 2003; Killiny and
407 Almeida 2009).

408 Significant decreases of proportion of infected insects, mean *Xf* load in insects alive at the end of
409 IAP, and survival rate were observed during autumn assays. Such trend could be explained by a
410 higher mortality of *Xf*-infected insects compared to healthy ones, especially under the stressing
411 conditions of the cages in semi-field conditions in autumn (colder climate and higher daily
412 temperature variations), when insects are old and approaching the end of their life. This
413 hypothesis would be consistent with the possible negative impact of *Xf* on fitness and survival of
414 the spittlebug, caused by the precibarium bacterial colonization and the consequent reduction of
415 available size of food canal. This reduction might lead to additional energy requirement to ingest
416 the xylem sap (Ranieri et al. 2020), and variations in feeding behaviour (e.g. shorter xylem
417 ingestion time and longer non-probing periods) (Cornara et al. 2020).

418 The transmission efficiency in the kinetics of *Xf* colonization experiment, i.e. the likelihood of
419 successful inoculation of *Xf* to olive, increased with bacterium population size in vectors, while it
420 was not significantly affected by the number of infected insects per inoculation batch, seasonal
421 dynamics of acquisition, and time post-acquisition during kinetic experiment. The transmission
422 efficiency by a batch composed by five *P. spumarius* was in average 34%, without significant
423 changes or trends overtime post-acquisition or among seasons. In other words, small groups of
424 vectors on single olive plant and controlled conditions inoculate at a constant rate, irrespective of

425 time post- acquisition and season. However, the increase of average *Xf* population per insect of
426 one order of magnitude (e.g. from 10^2 to 10^3 cells) led to a 3.2-fold increase of the likelihood of
427 olive infection. However, transmission efficiency at longer post-acquisition times (i.e. longer *Xf*
428 incubation time in vector's foregut), did not increase, likely because the positive correlation
429 between time post-acquisition and *Xf* load in *P. spumarius* was weak and there were insects with
430 high *Xf* populations in the foregut after few days post-acquisition and others with low number of
431 *Xf* cells after several weeks from acquisition. A positive correlation between transmission rate and
432 bacterial load in the vector was observed for the transmission of *X. fastidiosa* subsp. *fastidiosa* by
433 *P. spumarius* and *G. atropunctata* from grapevine to grapevine (Cornara et al. 2016; Zeilinger et
434 al. 2018).

435 The overall estimated average inoculation rate was 6% of infected plants per insect per day.
436 When considering the results obtained in different seasons, the inoculation rate per insect was
437 higher in autumn than in summer. In the literature, concerning *X. fastidiosa* subsp. *fastidiosa*,
438 higher inoculation rate estimates have been reported for *P. spumarius* and *G. atropunctata* on
439 grapevine (Cornara et al. 2016; Daugherty and Almeida 2009), similar for *Draeculacephala*
440 *minerva* Ball on periwinkle (Cabrera-La Rosa et al. 2008), and lower for *H. vitripennis* on
441 grapevine and almond (Almeida and Purcell 2003; Daugherty and Almeida 2009). According to
442 Marucci et al. (2008) and Lopes and Krugner (2016), inoculation efficiency of CVC strains of *X.*
443 *fastidiosa* subsp. *pauca* on citrus of main vector species [e.g. *Dilobopterus costalimai* Young,
444 *Acrogonia citrina* Marucci & Cavichioli, *Oncometopia facialis* (Signoret) and *Bucephalogonia*
445 *xanthophis* (Berg)] was lower or similar (1–13% over two-day IAP) to that estimated for *P.*
446 *spumarius* in this study. The inoculation rate of *P. spumarius* on olive calculated on data from
447 Cavalieri et al. (2019), 6–7% over four-day IAP, obtained with the Swallow formula (Swallow

448 1985), is lower compared to our estimate, 6% per day. However, the methodological differences
449 between the different studies — e.g. AAP and IAP duration, source plants, periods of the year,
450 statistical approaches adopted — suggest caution in comparing the outcomes of the different
451 studies. Moreover, in some studies, e.g. Daugherty and Almeida (2009), estimates were obtained
452 also reviewing datasets from several studies, whose methodologies were likely not homogeneous.
453 It is worth to point out that our estimates come from an experiment not specifically intended to
454 explore the effects of inoculation time and number of insect vectors per plant, being those
455 parameters fixed (3 days and 5 insects respectively), and thus are reliable for those conditions,
456 although the inoculation rate could vary with different combinations of inoculation duration and
457 number of inoculative insects (e.g. Daugherty and Almeida 2009; Cornara et al. 2016).

458 The epidemic spreading rate of *Xf* on olive by *P. spumarius*, i.e. the increase rate of the infected
459 plants proportion with inoculation time within an olive population, was affected by different
460 factors such as inoculum period, season and climatic conditions. Indeed, the spreading rate of *Xf*
461 was higher in controlled vs semi-field climatic conditions in all the assays, possibly meaning that
462 more stable climatic conditions — e.g. lower temperatures in summer and higher in autumn
463 assays compared to semi-field conditions or lower daily variations — resulted in a faster spread
464 of *Xf* among olive seedlings, possibly due to higher inoculation rates and/or higher mobility and
465 survival of *P. spumarius* in microcosms. Furthermore, the *Xf* spreading rate on olives increased
466 with inoculation time in autumn assays only, irrespective of climatic conditions. Although the
467 transmission rate is expected to increase with longer inoculation periods (Purcell and Finlay
468 1979; Daugherty and Almeida 2009; Cornara et al. 2016), also vector behaviour — e.g. the
469 preference for low water stressed plants — may influence host plant visiting, and ultimately the
470 transmission rate (Mizell et al. 2008; Del Cid et al. 2018). In our case, the observed seasonal

471 variation of *Xf* spreading rate on olive seedlings could be explained by a higher mobility of the
472 spittlebug in autumn, given that late in the season *P. spumarius* tends to move to herbaceous
473 species for mating and oviposition (Bodino et al. 2020a). Vector movement propensity may be
474 higher in this period, especially in a microcosm environment that does not provide good
475 oviposition sites, thus possibly forcing the vector to visit more olive seedlings. Finally, the *Xf*
476 spreading rate on olives was significantly higher in 2018 assays, when the vector density was
477 about double.

478 In summary, this work describes the influence of seasonal and environmental factors on the
479 transmission characteristics of *Xf* by *P. spumarius*. Such transmission dynamics could
480 significantly contribute to determine epidemic patterns in Apulian olive agroecosystem. The
481 highest rates of both acquisition and overall transmission of *Xf* in Apulian olive agroecosystem
482 occur probably in early summer, being the period with highest density of vectors on olive
483 canopies (Cornara et al. 2017b; Bodino et al. 2019, 2020a). However, because *P. spumarius* is
484 infectious throughout its adult life, our results indicate that transmission/spreading efficiency may
485 even increase in late season. Thus, the role of the spittlebug visiting olive canopies late in the
486 season could be epidemiologically relevant. Moreover, inoculation events taking place late in the
487 season could contribute to spread *Xf* at higher distances from the source plants, as the distance
488 travelled by an insect is a function of time, being in the range of 350-650 m after 5-6 months
489 from adult emergence in olive groves (Bodino et al. 2020b). Thus, older *P. spumarius* adults
490 could play a role in dispersing the bacterium at longer distances to olives or to wild plants within
491 the agroecosystem, expanding the infected area. Further studies on *Xf* spread in field or semi-field
492 condition, as well as on seasonal variations of dispersal and mobility of vectors are needed to
493 gain knowledge on factors driving the epidemic of *Xf* on olive. Besides transmission efficiency, *P.*

494 *spumarius* population level and preference for olive plants are major drivers of *Xf* spread in olive
495 groves. It is crucial to reduce populations of *P. spumarius* in olive groves in Apulia, since the
496 number of feeding insects is probably the most important factor determining successful
497 transmission and quick spread of the pathogen (Daugherty and Almeida 2009).

498 In conclusion, the transmission parameter estimates reported here, and their variation overtime,
499 should inform epidemic spread models of *Xf* in Italy and Europe that explicitly account for the
500 effect of vectors. *Philaenus spumarius* and its interactions with *Xf* in relation to spread are crucial
501 actors affecting the establishment, persistence, and epidemic spreading of the exotic pathogen
502 (Jeger and Bragard 2018).

503

504 **Author Contributions:** conceptualization, N.B., V.C., R.P.P.A., C.D., M.S., D.B.; methodology,
505 N.B., V.C., C.D., M.P., M.S., D.B.; data curation, N.B.; statistical analysis, N.B.; investigation,
506 N.B., V.C., C.D., F.C., M.P., G.A., S.Z., G.F.; resources, M.S., D.B.; writing—original draft
507 preparation, N.B.; writing—review and editing, N.B., V.C., C.D., F.C., M.S., R.P.P.A., D.B.;
508 supervision, D.B.; project administration, M.S., D.B.; funding acquisition, M.S., D.B.

509 **Funding:** This project has received funding from the European Union’s Horizon 2020 research
510 and innovation programme under grant agreement No 727987 “Xylella fastidiosa Active
511 Containment Through a multidisciplinary-Oriented Research Strategy XF-ACTORS”.

512 **Acknowledgments:** The authors wish to thank Elisa Plazio (CNR-IPSP Torino), for technical
513 support in the experiments; Francesco Palmisano and Antonella Saponari (Premultiplication
514 Center, CRSFA Basile Caramia) for the production of the recipient plants.

515 **Conflicts of Interest:** The authors declare no conflict of interest. The funders had no role in the
516 design of the study; in the collection, analyses, or interpretation of data; in the writing of the
517 manuscript, or in the decision to publish the results.

518

519 **References**

- 520 Abbott, A. (2018). Italy's olive crisis intensifies as deadly tree disease spreads. *Nature* 563(7731),
521 306–307. <https://doi.org/10.1038/d41586-018-07389-8>.
- 522 Allen, L.J.S., Bokil, V.A., Cunniffe, N.J., Hamelin, F.M., Hilker, F.M. & Jeger, M.J. (2019).
523 Modelling vector transmission and epidemiology of co-infecting plant viruses. *Viruses* 11(12),
524 1153. <https://doi.org/10.3390/v11121153>.
- 525 Almeida, R.P.P., Blua, M.J., Lopes, J.R.S. & Purcell, A.H. (2005). Vector transmission of *Xylella*
526 *fastidiosa*: applying fundamental knowledge to generate disease management strategies.
527 *Annual Entomology Society of America* 96(6), 775–786. [https://doi.org/10.1603/0013-](https://doi.org/10.1603/0013-8746(2005)098[0775:VTOXFA]2.0.CO;2)
528 [8746\(2005\)098\[0775:VTOXFA\]2.0.CO;2](https://doi.org/10.1603/0013-8746(2005)098[0775:VTOXFA]2.0.CO;2).
- 529 Almeida, R.P.P. & Purcell, A.H. (2003). Transmission of *Xylella fastidiosa* to grapevines by
530 *Homalodisca coagulata* (Hemiptera: Cicadellidae). *Journal of Economic Entomology* 96(2),
531 264–271. <https://doi.org/10.1093/jee/96.2.264>.
- 532 Anhalt, M.D. & Almeida, R.P.P. (2008). Effect of temperature, vector life stage, and plant access
533 period on transmission of banana bunchy top virus to banana. *Phytopathology* 98(6), 743–748.
534 <https://doi.org/10.1094/PHYTO-98-6-0743>.
- 535 Antonatos, S., Papachristos, D.P., Kapantaidaki, D.E., Lytra, I.C., Varikou, K., ... Milonas, P.
536 (2019). Presence of cicadomorpha in olive orchards of greece with special reference to *Xylella*
537 *fastidiosa* vectors. *Journal of Applied Entomology* 144(1–2), 1–11.
538 <https://doi.org/10.1111/jen.12695>.
- 539 Baccari, C. & Lindow, S.E. (2011). Assessment of the process of movement of *Xylella fastidiosa*
540 within susceptible and resistant grape cultivars. *Phytopathology* 101(1), 77–84.
541 <https://doi.org/10.1094/PHYTO-04-10-0104>.

542 Backus, E.A. & Shih, H.-T. (2020). Review of the EPG waveforms of sharpshooters and
543 spittlebugs including their biological meanings in relation to transmission of *Xylella fastidiosa*
544 (Xanthomonadales: *Xanthomonadaceae*). *Journal of Insect Science* 20(4), 1–14.
545 <https://doi.org/10.1093/jisesa/ieaa055>.

546 Bates, D., Mächler, M., Bolker, B. & Walker, S. (2015). Fitting linear mixed-effects models using
547 lme4. *Journal of Statistical Software* 67(1), 1–48. <https://doi.org/10.18637/jss.v067.i01>.

548 Bodino, N., Cavalieri, V., Dongiovanni, C., Plazio, E., Saladini, M.A., ... Bosco, D. (2019).
549 Phenology, seasonal abundance and stage-structure of spittlebug (Hemiptera: Aphrophoridae)
550 populations in olive groves in Italy. *Scientific Reports* 9(1), 17725.
551 <https://doi.org/10.1038/s41598-019-54279-8>.

552 Bodino, N., Cavalieri, V., Dongiovanni, C., Saladini, M.A., Simonetto, A., ... Bosco, D. (2020a).
553 Spittlebugs of Mediterranean olive groves: host-plant exploitation throughout the year. *Insects*
554 11(2), 130. <https://doi.org/10.3390/insects11020130>.

555 Bodino, N., Cavalieri, V., Dongiovanni, C., Simonetto, A., Saladini, M.A., ... Bosco, D. (2020b).
556 Dispersal of *Philaenus spumarius* (Hemiptera: Aphrophoridae), a vector of *Xylella fastidiosa*,
557 in olive grove and meadow agroecosystems. *Environmental Entomology* (nvaal140).
558 <https://doi.org/10.1093/ee/nvaa140>.

559 Cabrera-La Rosa, J.C., Johnson, M.W., Civerolo, E.L., Chen, J. & Groves, R.L. (2008). Seasonal
560 population dynamics of *Draeculacephala minerva* (Hemiptera: Cicadellidae) and transmission
561 of *Xylella fastidiosa*. *Journal of Economic Entomology* 101(4), 1105–1113.
562 <https://doi.org/10.1093/jee/101.4.1105>.

563 Cavalieri, V., Altamura, G., Fumarola, G., Carolo, M. di, Saponari, M., ... Dongiovanni, C.
564 (2019). Transmission of *Xylella fastidiosa* subspecies *pauca* sequence type 53 by different
565 insect species. *Insects* 10(10), 324. <https://doi.org/10.3390/insects10100324>.

566 Chatterjee, S., Almeida, R.P.P. & Lindow, S. (2008). Living in two worlds: the plant and insect
567 lifestyles of *Xylella fastidiosa*. *Annual Review of Phytopathology* 46(1), 243–271.
568 <https://doi.org/10.1146/annurev.phyto.45.062806.094342>.

569 Cornara, D., Bosco, D. & Fereres, A. (2018). *Philaenus spumarius*: when an old acquaintance
570 becomes a new threat to European agriculture. *Journal of Pest Science* 91(3), 957–972.
571 <https://doi.org/10.1007/s10340-018-0966-0>.

572 Cornara, D., Cavalieri, V., Dongiovanni, C., Altamura, G., Palmisano, F., ... Saponari, M.
573 (2017a). Transmission of *Xylella fastidiosa* by naturally infected *Philaenus spumarius*
574 (Hemiptera, Aphrophoridae) to different host plants. *Journal of Applied Entomology* 141(1–2),
575 80–87. <https://doi.org/10.1111/jen.12365>.

576 Cornara, D., Marra, M., Morente, M., Garzo, E., Moreno, A., ... Fereres, A. (2020). Feeding
577 behavior in relation to spittlebug transmission of *Xylella fastidiosa*. *Journal of Pest Science*
578 93, 1197–1213. <https://doi.org/10.1007/s10340-020-01236-4>.

579 Cornara, D., Morente, M., Markheiser, A., Bodino, N., Tsai, C.-W., ... Lopes, J.R.S. (2019). An
580 overview on the worldwide vectors of *Xylella fastidiosa*. *Entomologia Generalis* 39(3–4),
581 157–181. <https://doi.org/10.1127/entomologia/2019/0811>.

582 Cornara, D., Saponari, M., Zeilinger, A.R., Stradis, A. de, Boscia, D., ... Porcelli, F. (2017b).
583 Spittlebugs as vectors of *Xylella fastidiosa* in olive orchards in Italy. *Journal of Pest Science*
584 90(2), 521–530. <https://doi.org/10.1007/s10340-016-0793-0>.

585 Cornara, D., Sicard, A., Zeilinger, A.R., Porcelli, F., Purcell, A.H. & Almeida, R.P.P. (2016).
586 Transmission of *Xylella fastidiosa* to grapevine by the meadow spittlebug. *Phytopathology*
587 106(11), 1285–1290. <https://doi.org/10.1094/PHYTO-05-16-0202-R>.

588 Cruaud, A., Gonzalez, A.-A., Godefroid, M., Nidelet, S., Streito, J.-C., ... Rasplus, J.-Y. (2018).
589 Using insects to detect, monitor and predict the distribution of *Xylella fastidiosa*: a case study
590 in Corsica. *Scientific Reports* 8(1), 15628. <https://doi.org/10.1038/s41598-018-33957-z>.

591 Daugherty, M.P. & Almeida, R.P.P. (2009). Estimating *Xylella fastidiosa* transmission parameters:
592 decoupling sharpshooter number and feeding period. *Entomologia Experimentalis et Applicata*
593 132(1), 84–92. <https://doi.org/10.1111/j.1570-7458.2009.00868.x>.

594 Daugherty, M.P. & Almeida, R.P.P. (2019). Understanding how an invasive vector drives Pierce’s
595 disease epidemics: seasonality and vine-to-vine spread. *Phytopathology* 109(2), 277–285.
596 <https://doi.org/10.1094/PHYTO-07-18-0217-FI>.

597 Daugherty, M.P., Bosco, D. & Almeida, R.P.P. (2009). Temperature mediates vector transmission
598 efficiency: inoculum supply and plant infection dynamics. *Annals of Applied Biology* 155(3),
599 361–369. <https://doi.org/10.1111/j.1744-7348.2009.00346.x>.

600 Daugherty, M.P., Rashed, A., Almeida, R.P.P. & Perring, T.M. (2011). Vector preference for hosts
601 differing in infection status: sharpshooter movement and *Xylella fastidiosa* transmission.
602 *Ecological Entomology* 36(5), 654–662. <https://doi.org/10.1111/j.1365-2311.2011.01309.x>.

603 Daugherty, M., Zeilinger, A.R. & Almeida, R. (2017). Conflicting effects of climate and vector
604 behavior on the spread of a plant pathogen. *Phytobiomes* 1, 46–53.
605 <https://doi.org/10.1094/PBIOMES-01-17-0004-R>.

606 Del Cid, C., Krugner, R., Zeilinger, A.R., Daugherty, M.P. & Almeida, R.P.P. (2018). Plant water
607 stress and vector feeding preference mediate transmission efficiency of a plant pathogen.
608 *Environmental Entomology* 47(6), 1471–1478.

609 EFSA. (2018). Updated pest categorisation of *Xylella fastidiosa*. *EFSA Journal* 16(7), 1–61.
610 <https://doi.org/10.2903/j.efsa.2018.5357>.

611 EPPO. (2019). PM 7/24 (4) *Xylella fastidiosa*. *EPPO Bulletin* 49(2), 175–227.
612 <https://doi.org/10.1111/epp.12575>.

613 Esteves, M.B., Kleina, H.T., Sales, T. de M., Oliveira, T.P., Lara, I.A.R. de, ... Lopes, J.S. (2018).
614 Transmission efficiency of *Xylella fastidiosa* subsp. *pauca* sequence types by sharpshooter
615 vectors after in vitro acquisition. *Phytopathology* 109(2), 286–293.
616 <https://doi.org/10.1094/PHYTO-07-18-0254-FI>.

617 Freitag, J. (1951). Host range of the pierce’s disease virus of grapes as determined by insect
618 transmission. *Phytopathology* 41(10), 920–934.

619 Ghanim, M. (2014). A review of the mechanisms and components that determine the transmission
620 efficiency of tomato yellow leaf curl virus (Geminiviridae; Begomovirus) by its whitefly
621 vector. *Virus Research* 186, 47–54. <https://doi.org/10.1016/j.virusres.2014.01.022>.

622 Giampetruzzi, A., Baptista, P., Morelli, M., Cameirão, C., Lino Neto, T., ... Saldarelli, P. (2020).
623 Differences in the endophytic microbiome of olive cultivars infected by *Xylella fastidiosa*
624 across seasons. *Pathogens* 9(9), 723. <https://doi.org/10.3390/pathogens9090723>.

625 Gruber, B.R. & Daugherty, M.P. (2013). Understanding the effects of multiple sources of
626 seasonality on the risk of pathogen spread to vineyards: vector pressure, natural infectivity,
627 and host recovery. *Plant Pathology* 62(1), 194–204. [https://doi.org/10.1111/j.1365-](https://doi.org/10.1111/j.1365-3059.2012.02611.x)
628 [3059.2012.02611.x](https://doi.org/10.1111/j.1365-3059.2012.02611.x).

629 Harper, S.J., Ward, L.I. & Clover, G.R.G. (2010). Development of lamp and real-time pcr
630 methods for the rapid detection of *Xylella fastidiosa* for quarantine and field applications.
631 *Phytopathology* 100(12), 1282–1288. <https://doi.org/10.1094/PHYTO-06-10-0168>.

632 Hill, B.L. & Purcell, A.H. (1997). Populations of *Xylella fastidiosa* in plants required for
633 transmission by an efficient vector. *Phytopathology* 87(12), 1197–1201.
634 <https://doi.org/10.1094/PHYTO.1997.87.12.1197>.

635 Jeger, M.J. (2000). Theory and plant epidemiology. *Plant Pathology* 49(6), 651–658.
636 <https://doi.org/10.1046/j.1365-3059.2000.00522.x>.

637 Jeger, M.J., Bosch, F. van den, Madden, L.V. & Holt, J. (1998). A model for analysing plant-virus
638 transmission characteristics and epidemic development. *Mathematical Medicine and Biology: A Journal of the IMA* 15(1), 1–18. <https://doi.org/10.1093/imammb/15.1.1>.

640 Jeger, M.J. & Bragard, C. (2018). The epidemiology of *Xylella fastidiosa*; a perspective on
641 current knowledge and framework to investigate plant host-vector-pathogen interactions.
642 *Phytopathology* 109, 200–209. <https://doi.org/10.1094/PHYTO-07-18-0239-FI>.

643 Killiny, N. & Almeida, R.P.P. (2009). *Xylella fastidiosa* afimbrial adhesins mediate cell
644 transmission to plants by leafhopper vectors. *Applied and Environmental Microbiology* 75(2),
645 521–528. <https://doi.org/10.1128/AEM.01921-08>.

646 ~~Killiny, N., Rashed, A. & Almeida, R.P.P. (2012). Disrupting the transmission of a vector-borne
647 plant pathogen. *Applied and Environmental Microbiology* 78(3), 638–643.
648 <https://doi.org/10.1128/AEM.06996-11>.~~

649 Krugner, R. & Backus, E.A. (2014). Plant water stress effects on stylet probing behaviors of
650 *homalodisca vitripennis* (hemiptera: cicadellidae) associated with acquisition and inoculation
651 of the bacterium *Xylella fastidiosa*. *Journal of Economic Entomology* 107(1), 66–74.
652 <https://doi.org/10.1603/EC13219>.

653 Krugner, R., Hagler, J.R., Groves, R.L., Sisterson, M.S., Morse, J.G. & Johnson, M.W. (2012).
654 Plant water stress effects on the net dispersal rate of the insect vector *Homalodisca vitripennis*
655 (Hemiptera: Cicadellidae) and movement of its egg parasitoid, *Gonatocerus ashmeadi*
656 (Hymenoptera: Mymaridae). *Environmental Entomology* 41(6), 1279–1289.
657 <https://doi.org/10.1603/EN12133>.

658 Lopes, J. R. S. & Krugner, R. (2016). Transmission ecology and epidemiology of the citrus
659 variegated chlorosis strain of *Xylella fastidiosa*. In J. K. Brown (Ed.), *Vector-mediated*
660 *transmission of plant pathogens* (pp. 195-208). APS Press.

661 Mizell, R.F., Tipping, C., Andersen, P.C., Brodbeck, B.V., Hunter, W.B. & Northfield, T. (2008).
662 Behavioral model for *Homalodisca vitripennis* (Hemiptera: Cicadellidae): Optimization of
663 host plant utilization and management implications. *Environmental Entomology* 37(6), 1049–
664 1062.

665 Marucci, R.C., Lopes, J.R.S. & Cavichioli, R.R. (2008). Transmission efficiency of *Xylella*
666 *fastidiosa* by sharpshooters (Hemiptera: Cicadellidae) in coffee and citrus. *Journal of*
667 *Economic Entomology* 101(4), 1114–1121. <https://doi.org/10.1093/jee/101.4.1114>.

668 Morente, M., Cornara, D., Plaza, M., Durán, J.M., Capiscol, C., ... Fereres, A. (2018).
669 Distribution and relative abundance of insect vectors of *Xylella fastidiosa* in olive groves of
670 the Iberian peninsula. *Insects* 9(4), 175. <https://doi.org/10.3390/insects9040175>.

671 Newman, K.L., Almeida, R.P.P., Purcell, A.H. & Lindow, S.E. (2004). Cell-cell signaling controls
672 *Xylella fastidiosa* interactions with both insects and plants. *Proceedings of the National*
673 *Academy of Sciences of the United States of America* 101(6), 1737–1742.
674 <https://doi.org/10.1073/pnas.0308399100>.

675 Pinheiro, J., Bates, D., DebRoy, S., Sarkar, D., & R Core Team. (2020). *nlme: Linear and*
676 *Nonlinear Mixed Effects Models*.

677 Purcell, A.H. (1981). Vector preference and inoculation efficiency as components of resistance to
678 pierce's disease in European grape cultivars. *Phytopathology* 71(4), 429–435.

679 Purcell, A.H. & Almeida, R.P.P. (2005). Insects as vectors of disease agents. In R. M. Goodman
680 (Ed.), *Encyclopedia of Plant and Crop Science* (pp. 1–10). CRC Press.
681 <https://doi.org/10.1081/E-EPCS>.

682 Purcell, A.H. & Finlay, A. (1979). Evidence for noncirculative transmission of Pierce's disease
683 bacterium by sharpshooter leafhoppers. *Phytopathology* 69(4), 393.
684 <https://doi.org/10.1094/Phyto-69-393>.

685 R Core Team. (2020). *R: A Language and Environment for Statistical Computing*. R Foundation
686 for Statistical Computing, Vienna, Austria.

687 Ranieri, E., Zitti, G., Riolo, P., Isidoro, N., Ruschioni, S., ... Almeida, R.P.P. (2020). Fluid
688 dynamics in the functional foregut of xylem-sap feeding insects: a comparative study of two
689 *Xylella fastidiosa* vectors. *Journal of Insect Physiology* 120, 103995.
690 <https://doi.org/10.1016/j.jinsphys.2019.103995>.

691 Redak, R.A., Purcell, A.H., Lopes, J.R.S., Blua, M.J., Mizell III, R.F. & Andersen, P.C. (2004).
692 The biology of xylem fluid-feeding insect vectors of *Xylella fastidiosa* and their relation to
693 disease epidemiology. *Annual Review of Entomology* 49(1), 243–270.
694 <https://doi.org/10.1146/annurev.ento.49.061802.123403>.

695 Roper, C., Castro, C. & Ingel, B. (2019). *Xylella fastidiosa*: bacterial parasitism with hallmarks of
696 commensalism. *Current Opinion in Plant Biology* 50, 140–147.
697 <https://doi.org/10.1016/j.pbi.2019.05.005>.

698 Saponari, M., Boscia, D., Altamura, G., Loconsole, G., Zicca, S., ... Martelli, G.P. (2017).
699 Isolation and pathogenicity of *Xylella fastidiosa* associated to the Olive Quick Decline
700 Syndrome in Southern Italy. *Scientific Reports* 7(1), 17723. [https://doi.org/10.1038/s41598-](https://doi.org/10.1038/s41598-017-17957-z)
701 [017-17957-z](https://doi.org/10.1038/s41598-017-17957-z).

702 Saponari, M., Giampetruzzi, A., Loconsole, G., Boscia, D. & Saldarelli, P. (2019). *Xylella*
703 *fastidiosa* in olive in Apulia: where we stand. *Phytopathology* 109(2), 175–186.
704 <https://doi.org/10.1094/PHYTO-08-18-0319-FI>.

705 Schneider, K., Werf, W. van der, Cendoya, M., Mourits, M., Navas-Cortés, J.A., ... Lansink, A.O.
706 (2020). Impact of *Xylella fastidiosa* subspecies *pauca* in European olives. *Proceedings of the*
707 *National Academy of Sciences*. <https://doi.org/10.1073/pnas.1912206117>.

708 Severin, H.H.P. (1950). Spittle-insect vectors of pierce's disease virus. ii. life history and virus
709 transmission. *Hilgardia* 19, 357–376.

710 Sicard, A., Zeilinger, A.R., Vanhove, M., Schartel, T.E., Beal, D.J., ... Almeida, R.P.P. (2018).
711 *Xylella fastidiosa*: insights into an emerging plant pathogen. *Annual Review of Phytopathology*
712 56(1), 181–202. <https://doi.org/10.1146/annurev-phyto-080417-045849>.

713 Strona, G., Castellano, C., Fattorini, S., Ponti, L., Gutierrez, A.P. & Beck, P.S.A. (2020). Small
714 world in the real world: long distance dispersal governs epidemic dynamics in agricultural
715 landscapes. *Epidemics* 30, 100384. <https://doi.org/10.1016/j.epidem.2020.100384>.

716 Swallow, W.H. (1985). Group testing for estimating infection rates and probabilities of disease
717 transmission. *Phytopathology* 75(8), 882–889.

718 White, S.M., Bullock, J.M., Hooftman, D.A.P. & Chapman, D.S. (2017). Modelling the spread
719 and control of *Xylella fastidiosa* in the early stages of invasion in Apulia, Italy. *Biological*
720 *Invasions 1825–1837*, 1825–1837. <https://doi.org/10.1007/s10530-017-1393-5>.

721 White, S.M., Navas-Cortés, J.A., Bullock, J.M., Boscia, D. & Chapman, D.S. (2020). Estimating
722 the epidemiology of emerging *Xylella fastidiosa* outbreaks in olives. *Plant Pathology* 69(8),
723 1403–1413. <https://doi.org/10.1111/ppa.13238>.

724 Wickham, H. (2016). *ggplot2: Elegant Graphics for Data Analysis*. Springer-Verlag New York.

725 Zeilinger, A.R., Turek, D., Cornara, D., Sicard, A., Lindow, S.E. & Almeida, R.P.P. (2018).
726 Bayesian vector transmission model detects conflicting interactions from transgenic disease-
727 resistant grapevines. *Ecosphere* 9(11), e02494. <https://doi.org/10.1002/ecs2.2494>.

728

729 **Figure legends**

730 **Figure 1:** Proportion of *Xf*-positive *Philaenus spumarius* individuals at different timepoints after
731 acquisition from infected olive branches during Summer and Autumn 2017-2018 assays. Hollow
732 points represent result of single insects (positive = 1, negative = 0), a small amount of variation
733 was included to make visible the number of insects tested at each timepoint even if the multiple
734 points had the exact same value. Red filled points and line represent proportion of positive insects
735 (mean + SE) and the red lines the outcome of binomial GLMM model; data from insects
736 collected immediately after AAP end were excluded from depicted GLMM model, to avoid
737 biased estimation of infected insects.

Figure 2: PCR-estimated population of *Xf* in *Philaenus spumarius* foregut (decimal log-
transformed no. of cells) at different timepoints after acquisition from infected olive branches
during Summer and Autumn 2017-2018 assays. Hollow points represent result of single positive
insects, red filled points represent proportion of positive insects (mean + SE), continuous black
lines the outcome of Michaelis-Menten model and dashed grey line the outcome of linear model.

738

739 **Figure 3:** Proportion of *Xf*-positive olive seedlings inoculated by batches ($n = 5$) of *Philaenus*
740 *spumarius* at different timepoints after acquisition from infected olive branches during Summer
741 and Autumn 2017-2018 assays. Hollow triangles represent result of single plants (positive = 1,
742 negative = 0), a small amount of variation was included to make visible the number of plants
743 tested at each timepoint even if the multiple points had the exact same value. Green filled points
744 represent the proportion of positive olive plantlets (mean + SE) and the green lines represent the
745 outcome of binomial GLM model described in Table 1.

746

747 **Figure 4:** Proportion of *Xf*-positive olive plantlets related with mean *Xf* population size (decimal
748 log of no. of cells) in *Philaenus spumarius* inoculation batches. Hollow points represent result of
749 single plants (positive = 1, negative = 0), a small amount of variation was included to make
750 visible the number of plants tested even if the multiple points had the exact same value. Red
751 filled points represent the proportion of *Xf*-positive olive plantlets for each binned log span of
752 mean *Xf* population size in *P. spumarius* inoculation batch. Red line represents the outcome of
753 binomial GLMM model.

754

Figure 5: Proportion of *Xf*-positive *Philaenus spumarius* individuals after different inoculation
periods in *Xf* spread experiments during Summer and Autumn 2017-2018 assays. Note that x-axis
scale is equal to IAP duration + 3 days of AAP). Hollow points represent result of single insects
(positive = 1, negative = 0), a small amount of variation was included to make visible the number
of insects tested at each timepoint even if the multiple points had the exact same value. Filled
points and triangles represent proportion of positive insects (mean + SE) recollected at different
IAPs and the lines the outcome of binomial GLMM model from different climatic conditions. A
small amount of horizontal variation was included for points and triangles to avoid overlap.

755

Figure 6: PCR-estimated population of *Xf* in *Philaenus spumarius* foregut (decimal log-
transformed no. of cells) of individuals recollected alive at the end of IAPs in *Xf* spread
experiments during Summer and Autumn 2017-2018 assays. Note that x-axis scale is equal to
IAP duration + 3 days of AAP). Hollow points represent result of single insects. Filled points and

triangles represent the mean (\pm SE) number of *Xf* cells in recollected *P. spumarius* at different IAPs and the lines the outcome of linear regression model from different climatic conditions.

756

Figure 7: Proportion of infected olive seedling after different inoculation periods in *Xf* spread experiments during Summer and Autumn 2017-2018 assays. Points and triangles represent proportion of positive insects (mean + SE) and the continuous and dashed lines the outcome of binomial GLMM model from different climatic conditions (points-continuous lines = controlled; triangles-dashed lines = natural).

757

758

759 **Tables**

Table 1: Estimated odds ratios, z-statistics significance and confidence interval (95%) from a logistic GLMM of fixed covariates *Time post-acquisition*, *Season* and its interaction on proportion of infected *Philaenus spumarius* and proportion of infected olive seedlings in kinetic experiment.

	PCR-positive insects	Plants infected
Time post-AAP	1.01 (1.00 – 1.02)	0.99 (0.97 – 1.02)
Season	4.95 *** (2.84 – 8.62)	0.93 (0.20 – 4.34)
Time post-AAP x Season	0.95 ** (0.92 – 0.99)	1.03 (0.96 – 1.12)
N	538	82
N (Year)	2	2
SD (Year)	0.63	0
BIC	720.49	126.79
R2 (fixed)	0.08	0.03
R2 (total)	0.18	0.03

760

761

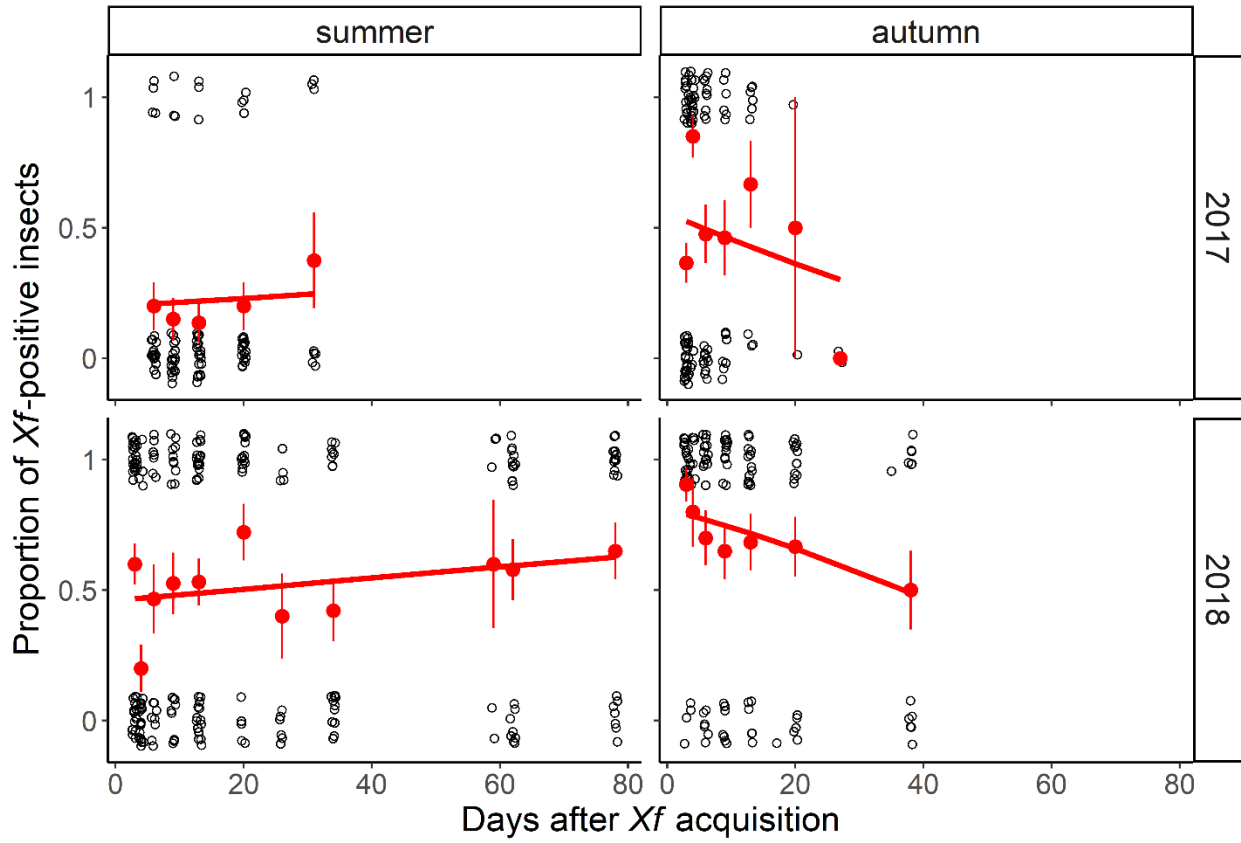
Table 2: Estimated parameters from a logistic GLMM or linear regression of fixed covariates *Inoculation duration, Climatic condition, Season* and *Year* on proportion of infected *Philaenus spumarius, Xylella fastidiosa* population size at the end of IAP in collected individuals and proportion of infected olive seedlings in spread rate experiment.

	Survival rate	PCR-positive insects ^a	<i>Xf</i> population (pos + neg) ^b	Plants infected ^a
IAP duration	0.93 *** (0.91 – 0.95)	0.97 (0.92 – 1.01)	-0.13 *** (-0.20 – -0.06)	1.02 (0.97 – 1.06)
Climatic conditions	5.99 *** (3.74 – 9.58)	1.38 (0.69 – 2.77)	0.60 (-0.59 – 1.79)	10.89 ** (2.48 – 47.80)
Season	1.94 ** (1.31 – 2.89)	8.09 *** (3.43 – 19.07)	1.84 ** (0.70 – 2.98)	0.57 (0.25 – 1.30)
Year	—	—	—	34.54 *** (8.20 – 145.47)
IAP duration x Climatic conditions	1.00 (0.97 – 1.03)	1.01 (0.95 – 1.07)	0 (-0.09 – 0.08)	—
IAP duration x Season	0.87 *** (0.84 – 0.90)	0.86 ** (0.77 – 0.96)	-0.08 (-0.20 – 0.03)	1.08 ** (1.02 – 1.15)
Season x Climatic conditions	0.29 *** (0.19 – 0.43)	0.19 ** (0.06 – 0.56)	-1.47 (-2.97 – 0.04)	—
Climatic conditions x Year	—	—	—	0.13 * (0.03 – 0.63)
IAP duration x Climatic conditions x SeasonAutmn	—	1.21 ** (1.07 – 1.38)	0.23 ** (0.07 – 0.38)	—
N	96	829	704	1489
N (replica)	—	3	—	—
N (year)	2	—	—	96
BIC	530.96	1126.39	3545.95	928.86
R2 (fixed)	0.38	0.11	—	0.43
R2 (total)	0.42	0.11	0.18	0.45

762 ^aLogistic GLMM, estimated odds ratios, z-statistics significance and confidence interval (95%)

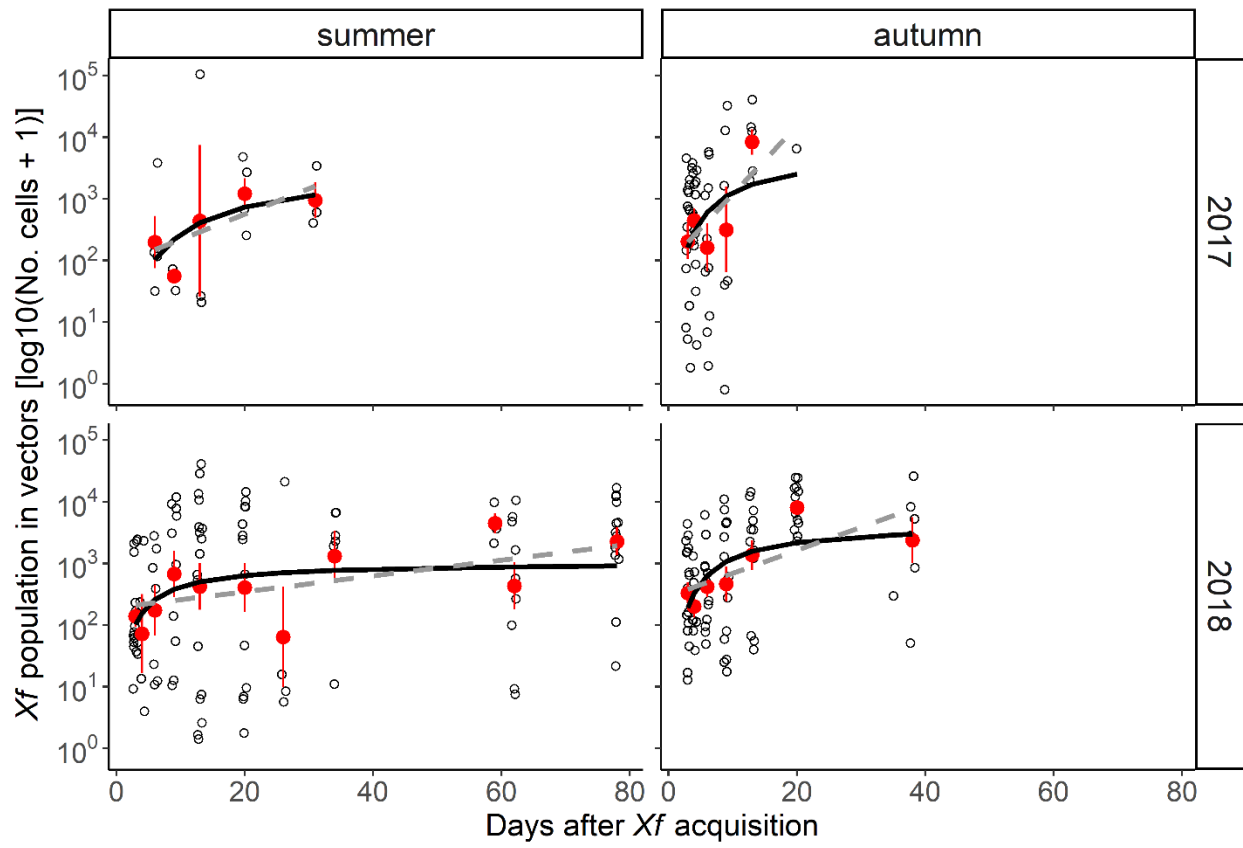
763 ^bLinear regression, estimated intercept and slope parameters, t-statistics significance and confidence interval (95%)

Figure 1



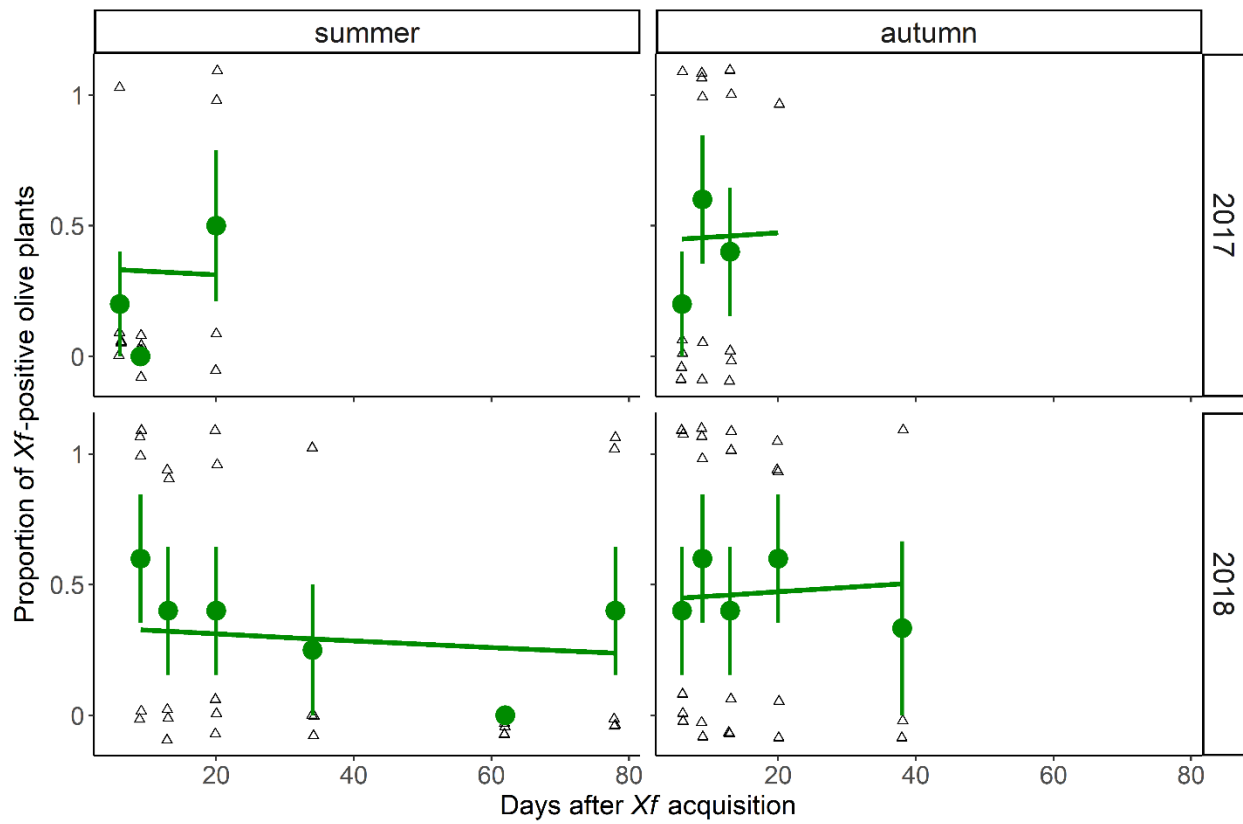
765
766

767 **Figure 2**



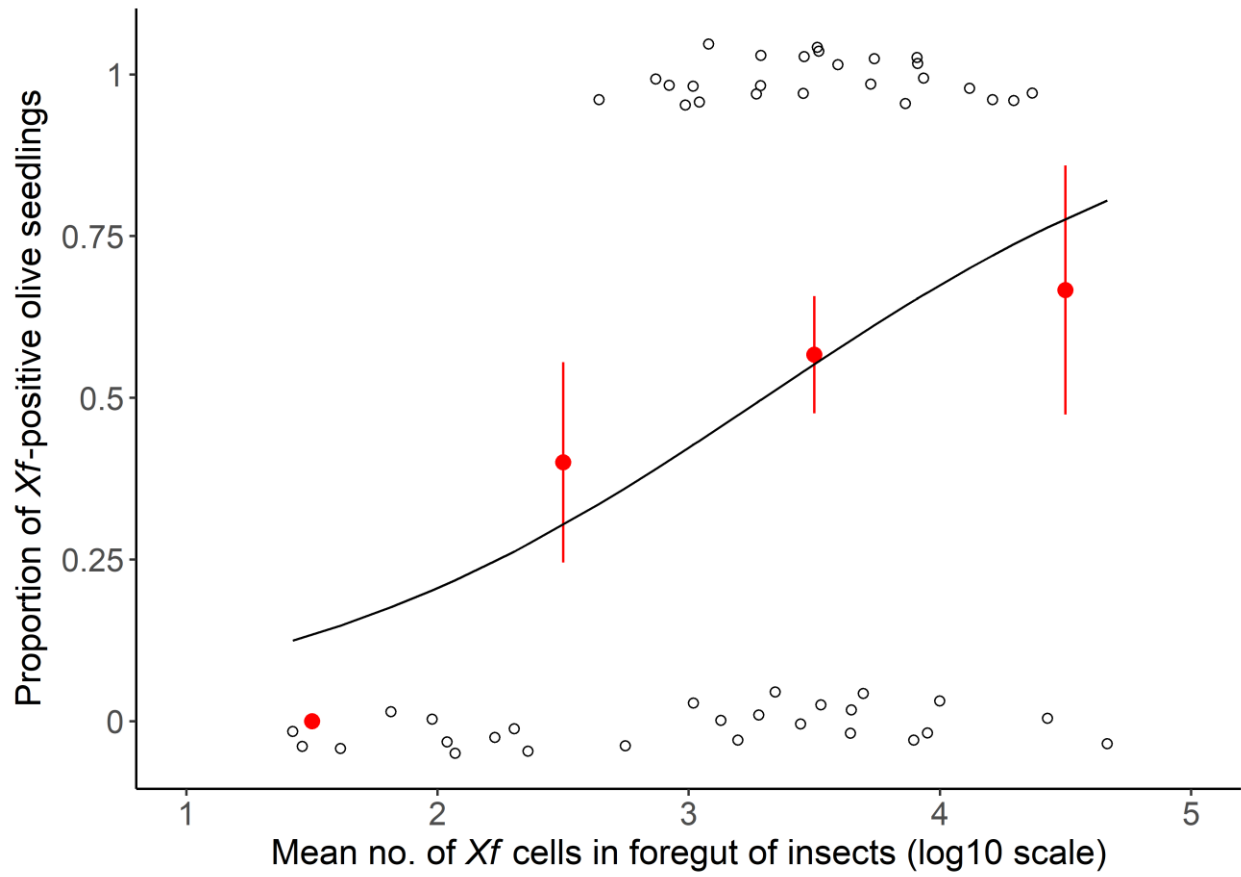
768
769

770 **Figure 3**



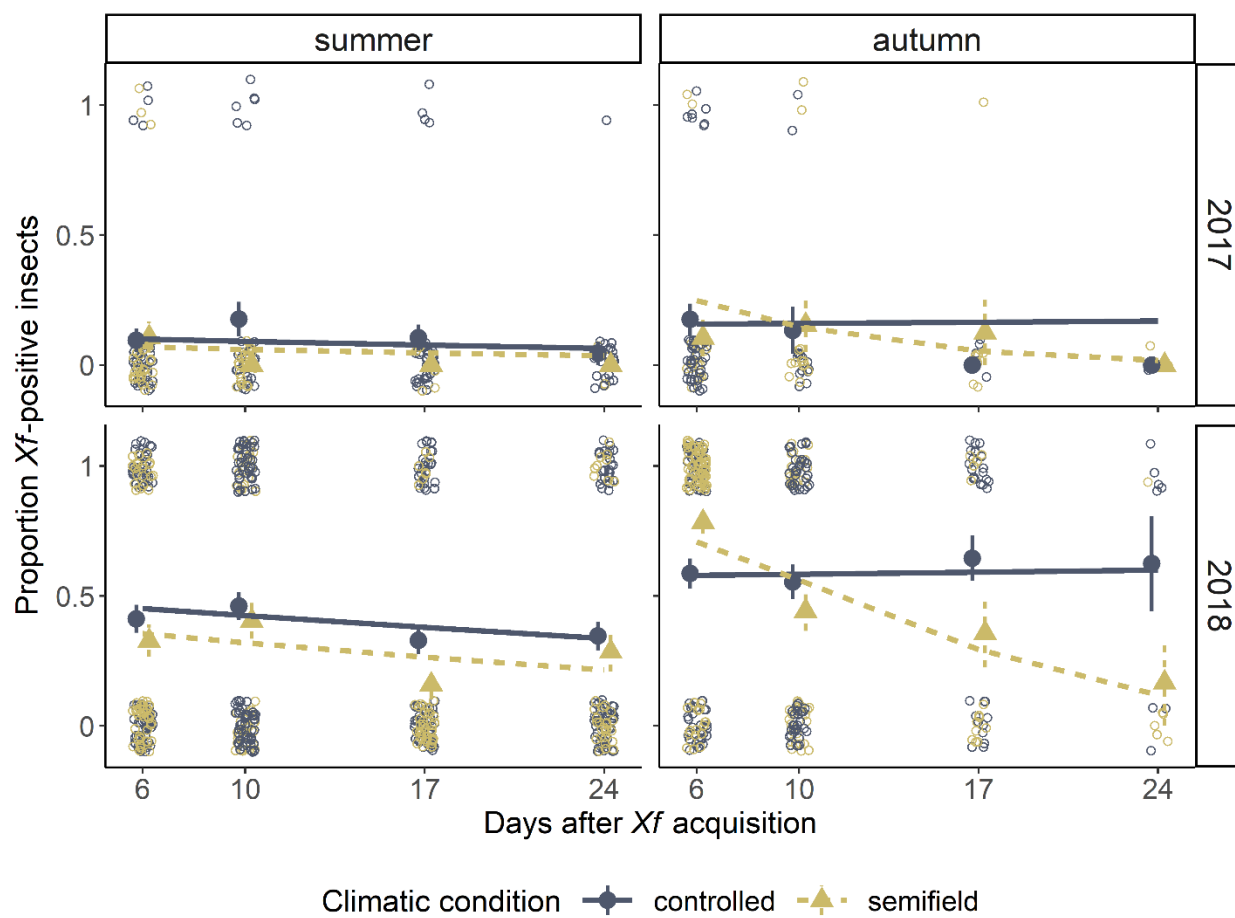
771
772

773 **Figure 4**



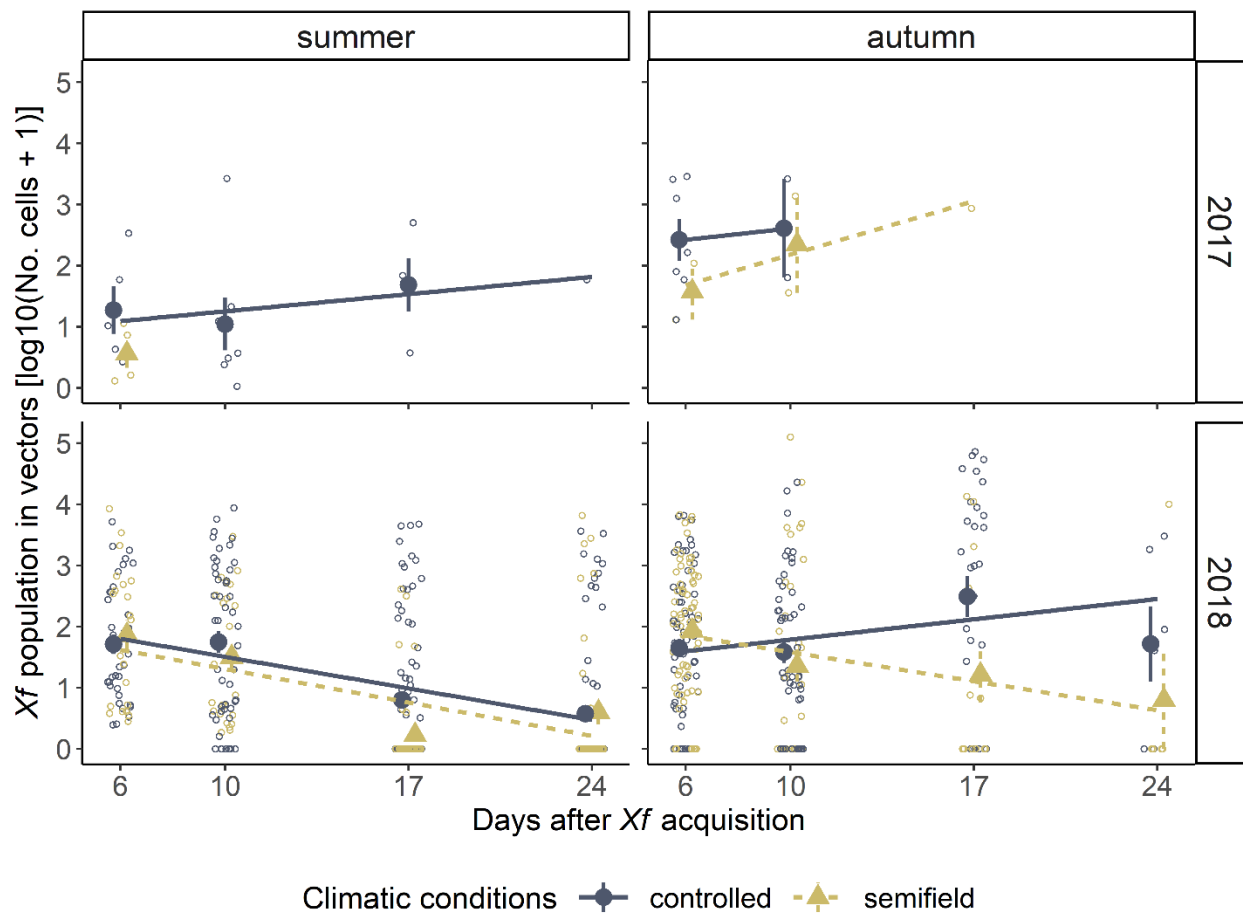
774
775

776 **Figure 5**



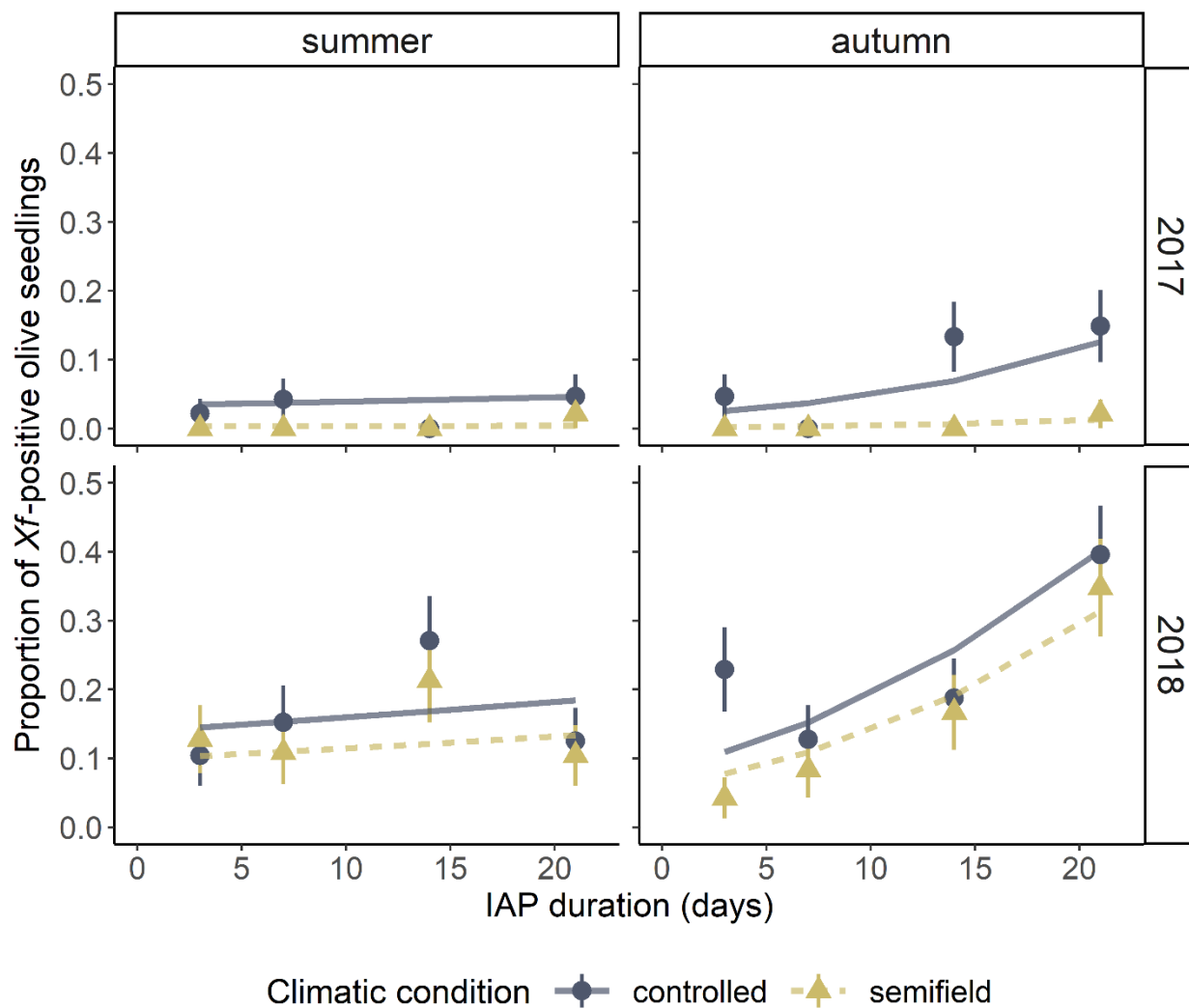
777
778

779 **Figure 6**



780
781

782 **Figure 7**



783